Molecular Vision **1999; 5:20** <http://www.molvis.org/molvis/v5/p20>
Received 29 June 1999 | Accepted 3 September 1999 | Published 3 September 1999

Aldose and aldehyde reductases: Structure-function studies on the coenzyme and inhibitor-binding sites

Ossama El-Kabbani,[1] Susan E. Old,[2] Stephan L. Ginell,[3]Deborah A. Carper[2]

[1]Department of Medicinal Chemistry, Victorian College of Pharmacy, Monash University, Parkville, Australia; [2]National Eye Institute, National Institutes of Health, Bethesda, MD, USA; [3]Structural Biology Center, Argonne National Laboratory, Argonne, IL, USA

Purpose: To identify the structural features responsible for the differences in coenzyme and inhibitor specificities of aldose and aldehyde reductases.
Methods: The crystal structure of porcine aldehyde reductase in complex with NADPH and the aldose reductase inhibitor sorbinil was determined. The contribution of each amino acid lining the coenzyme-binding site to the binding of NADPH was calculated using the Discover package. In human aldose reductase, the role of the non-conserved Pro 216 (Ser in aldehyde reductase) in the binding of coenzyme was examined by site-directed mutagenesis.
Results: Sorbinil binds to the active site of aldehyde reductase and is hydrogen-bonded to Trp 22, Tyr 50, His 113, and the non-conserved Arg 312. Unlike tolrestat, the binding of sorbinil does not induce a change in the side chain conformation of Arg 312. Mutation of Pro 216 to Ser in aldose reductase makes the binding of coenzyme more similar to that of aldehyde reductase.
Conclusions: The participation of non-conserved active site residues in the binding of inhibitors and the differences in the structural changes required for the binding to occur are responsible for the differences in the potency of inhibition of aldose and aldehyde reductases. We report that the non-conserved Pro 216 in aldose reductase contributes to the tight binding of NADPH.

Aldehyde reductase (ALR1; EC 1.1.1.2) and aldose reductase (ALR2; EC 1.1.1.21), members of the aldo-keto reductase superfamily, are monomeric, primarily NADPH-dependent oxidoreductases that catalyze the reduction of a wide variety of aldehydes and ketones to their corresponding alcohols [1]. Despite considerable research, a physiological role for the enzymes has not yet been identified. However, the ability of ALR2 to reduce excess glucose to sorbitol in diabetes mellitus has implicated the enzyme in the pathogenesis of diabetic complications affecting the eyes, kidneys, and nervous system [2]. To date, none of the currently available aldose reductase inhibitors (ARIs) has proved clinically effective and some have had deleterious side effects [3]. Nevertheless, the therapeutic rationale for using inhibitors to delay the onset and/or progression of diabetic retinopathy and neuropathy is still considered valid [4]. Although there are no reports of inhibitors that have been developed to specifically inhibit ALR1, biochemical studies have shown that many ARIs inhibit ALR1 [5].

Crystallographic analyses of ALR1 [6,7] and ALR2 [8] have shown that the three-dimensional structures of the enzymes are composed of similar α/β TIM-barrels. The coenzyme NADPH is bound in an extended conformation with the nicotinamide moiety positioned to allow a hydride transfer from the C-4 atom to the carbonyl group of the substrate while a proton is provided by the enzyme [7,8]. The pyrophosphate bridge of NADPH is tied down by loop B (residues 214-230), holding NADPH tightly in place, and loop B is fastened by the interaction of Asp 217 with lysine residues 23 and 263 [7,8]. We have recently reported the structure of ALR1 holoenzyme in complex with the carboxylic acid inhibitor tolrestat and we have shown that tolrestat binding induces a conformational change in the non-conserved Arg 312 [9]. In this study we show that unlike tolrestat, the binding of the spirohydantoin inhibitor sorbinil to ALR1 is not accompanied by a conformational change in the enzyme, and indicate reasons why sorbinil inhibits both ALR1 and ALR2 with similar potencies while tolrestat is a more potent inhibitor of ALR2 than ALR1 [10]. In addition, we show that the non-conserved Pro 216 (Ser in ALR1) contributes to the tighter binding of coenzyme to ALR2 [11,12].

METHODS

X-ray crystallography: Hexagonal crystals of the porcine ALR1 holoenzyme were grown from buffered ammonium sulfate solutions as described earlier [7] and soaked in synthetic mother liquor containing 1 mM sorbinil, $C_{11}H_9FN_2O_3$, for two days. High resolution data (1.99 Å) were collected from one flash frozen crystal at -165 °C using the 3,072 x 3,073 pixel CCD electronic area detector [13] at the Argonne National Laboratory Structural Biology Center at beamline X8C of the National Synchrotron Light Source, Brookhaven National Laboratory, Upton, NY. Data frames were collected for 100 s using a 0.2°phi scans at a crystal to detector distance

Correspondence to: Ossama El-Kabbani, Ph.D., Department of Medicinal Chemistry, Victorian College of Pharmacy, Monash University (Parkville Campus), 381 Royal Parade, Parkville, Vic 3052, Australia; Phone: 61 3 9903 9691; Fax: 61 3 9903 9582; e-mail: ossama.el-kabbani@vcp.monash.edu.au

of 297 mm and a wavelength of 1.00615 Å. The data were processed using MADNESS [14] to a final set of 21,592 out of 22,580 possible unique reflections at 1.99 Å resolution with an overall R_{merge} of 0.03 and $\mathbf{I}/\sigma(\mathbf{I})$=59. The crystal form is hexagonal, space group $P6_522$ with a=b=66.75 Å, c=245.68 Å, α=β=90.0°and γ=120.0°. The value for V_m is 2.24 Å Da^{-1} for a solvent content of 45%, and one molecule per asymmetric unit. The sorbinil-binding site and the positions of 336 water molecules were located from a difference electron density map calculated with phases derived from the model of the binary complex (Figure 1) using the computer program TOM (the IRIS version of FRODO [15]) and an SGI Indigo XZ computer graphics system (Silicon Graphics, Mountain View, CA). The structure was refined using the slow cooling protocol of X-PLOR [16] and the 19,204 reflections between 6.0 Å and 2.0 Å resolution with $\mathbf{I}>2.0\sigma(\mathbf{I})$ (98.4% of the observed unique reflections). The final refinement produced an R-factor of 0.18 and a root-mean-square deviation (r.m.s.d.) of bond lengths and bond angles from ideality of 0.009 and 2.1°, respectively. The PDB entry number is pending for the atomic coordinates for the porcine ALR1 holoenzyme-sorbinil complex.

Molecular modeling calculations: The high resolution crystal coordinates of human aldose reductase and porcine aldehyde reductase holoenzymes including crystallographic waters (Brookhaven Protein Data Bank Entries 1ADS and 1CWN) were used in the present modeling study (crystal coordinates of porcine aldose reductase holoenzyme in complex with sorbinil were not available during the study). Hydrogen atoms, partial charges, atomic potentials, and bond orders were assigned using the automatic procedures within the Insight II package (Biosym Technologies Inc., San Diego, CA). Arginine, lysine, aspartate, and glutamate amino acid residues were charged while the histidines were uncharged, with hydrogen atoms fixed at the Nε atoms. Energy minimizations were performed to relieve steric strain associated with the crystal coordinates using the Discover package (Biosym Technologies Inc., San Diego, CA) on an O2 (R10000) workstation (Silicon Graphics, Mountain View, CA). Calculations were done using the algorithms steepest descents and conjugate gradients (down to a maximum atomic root mean square derivative of 10.0 kcal/Å and 0.01 kcal/Å, respectively). The energy minimized structures were visualized using Insight II and the contribution of each amino acid residue adjacent to the coenzyme to the binding energy in ALR1 and ALR2 was calculated using Discover.

Generation of mutant protein: Mutant human ALR2, P216S, was generated using the PCR recombinant circle technique [17]. Proline with the codon CCT was replaced with the serine codon TCT. PCR was performed as previously described [18] using 70 ng of the human ALR2 DNA as template [19]. The reaction sample was denatured for 3 min at 95 °C followed by a 2 min annealing step at 65 °C. VENT polymerase (New England Biolabs, Beverly, MA) was then added and an initial extension was for 8 min at 70 °C. Amplification was carried out for 14 cycles (1 min at 95 °C, 30 s at 65 °C and 8 min at 70 °C) followed by a final extension for 10 min at 70 °C. The PCR products were annealed and transfected into *E. coli* strain BL21(DE3) cells (Novagen, Madison, WI). One clone was selected and completely sequenced to verify that only the intended mutation was present.

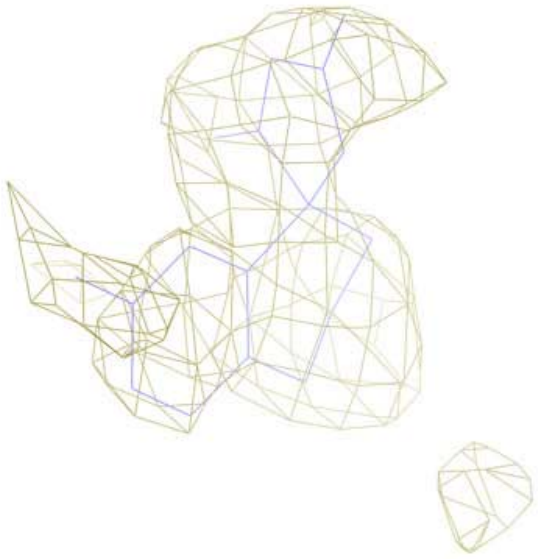

Figure 1. Sorbinil (blue) with superimposed electron density (yellow). The density was calculated with sorbinil excluded from the model using coefficients ($\mathbf{F}_o$-$\mathbf{F}_c$) and α_c. The average temperature factor for all sorbinil atoms refined at 2.0 Å resolution is 35. The density shown at lower right corresponds to a water molecule.

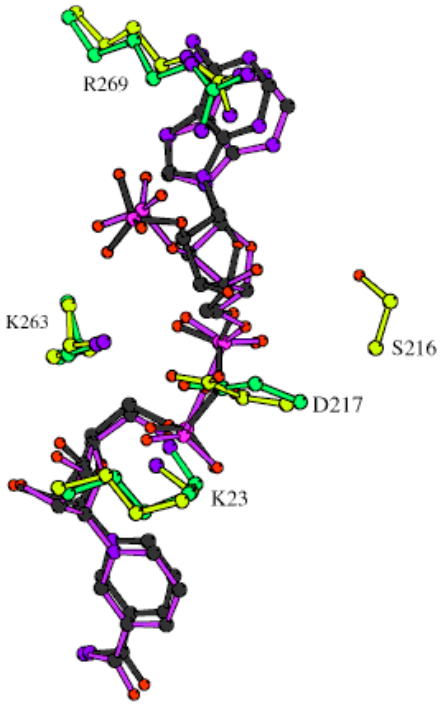

Figure 2. Superimposed coenzyme-binding sites of ALR1 and ALR2. For clarity only residues Lys 23, Ser 216, Asp 217, Lys 263, and Arg 269 with bound coenzyme are shown for ALR1 (amino acid side chains in yellow, coenzyme in magenta) and ALR2 (amino acid side chains in green, coenzyme in black). Atomic coordinates for the ALR2 residues were obtained from the Brookhaven Protein Data Bank (entry 1ADS).

ALR2 wildtype and mutant proteins were generated from 1 L preparations of bacterial cells containing either the wildtype or mutant ALR2 plasmid using methods previously described [19]. ALR2 was purified from the bacterial cell supernatant using a Sephadex G-75 column (Pharmacia, Piscataway, NJ) followed by separation on a MonoP chromatofocusing column (Pharmacia). The eluted ALR2 protein was evaluated by SDS polyacrylamide gel electrophoresis (Phastsystem, Pharmacia), and the protein concentration was quantified using the Bradford method [20].

The dissociation constants, K_d, for NADPH and $NADP^+$ were determined by measuring the quenching of the intrinsic protein fluorescence (excitation 295 nm: emission 340 nm) using an Aminco 500 fluorescence spectrophotometer (SLM Instruments, Urbana, IL). Nucleotide-free enzyme preparations were titrated with the sequential addition of cofactor as previously described [19]. To produce nucleotide-free enzyme, NaCl was added to the purified enzymes to yield a final concentration of 0.5 M. After 30 min, the samples were then passed through two consecutive PD10 Sephadex G-25 columns (Pharmacia, Sweden) equilibrated with 5 mM sodium phosphate buffer, pH 7.0, containing 100 µM DTT. K_d values were determined as described [18, 19].

Enzyme activity was measured during purification of ALR2 by monitoring the decrease in NADPH absorbance at 340 nm in a Shimadzu model UV-160 spectrophotometer (Shimadzu Scientific Instruments, Columbia, MD) as previously described [18]. Kinetic constants were calculated using Hypercard software (D.G. Gilbert, Indiana University, Bloomington, IN).

Table 1. Intermolecular binding enthalpies (kcal/mol) between ALR1 and ALR2 and NADPH

Protein residue[a]	ALR1 ΔH (kcal/mol)	ALR2 ΔH (kcal/mol)
Thr 21	-2	-2
Trp 22	-10	-9
Asp 45	-23	-22
Tyr 50	-6	-5
His 113	-5	-4
Trp 114	-1	-2
Asn 163	-1	-3
Gln 184	-4	-7
Tyr 210	-11	-11
Ser 211	-10	-10
Pro 212	-2	-3
Leu 213	-8	-8
Ser 215	-7	-8
Ser 216 (Pro)	-6	-4
Asp 217	-4	-20
Leu 229	-3	-3
Thr 266	-1	-2
Ala 246	-2	-2
Ile 261	-4	-4
Pro 262	-3	-3
Lys 263	-15	-12
Ser 264	-4	-4
Val 265	-3	-4
Arg 269	-13	-16
Gln 272 (Glu)	-1	-2
Asn 273	-4	-3
Ile 299 (Val)	-3	-1
Total protein energy	-170	-189

[a]The corresponding non-conserved residues in ALR2 are shown in brackets.

RESULTS & DISCUSSION

Coenzyme-binding site: The coenzyme NADPH bound to

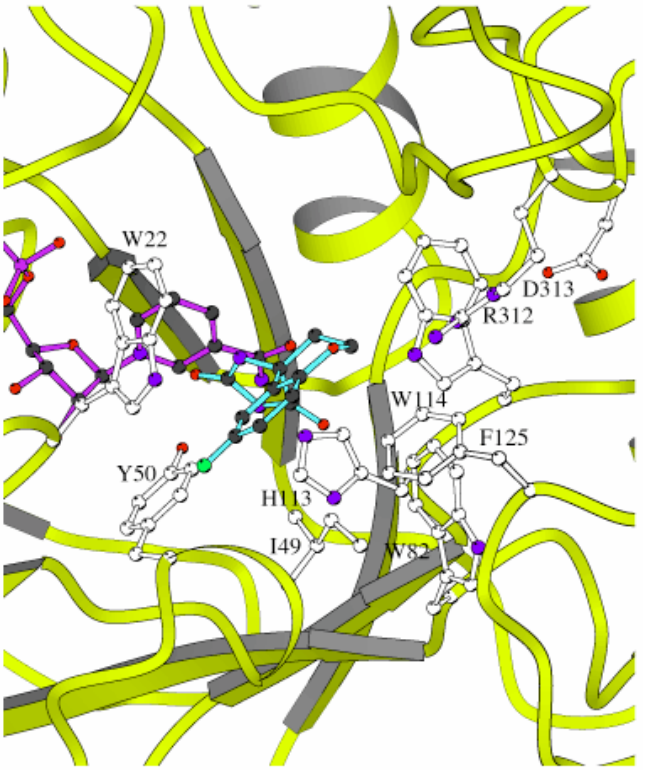

Figure 3. Inhibitor-binding site for porcine ALR1. Amino acid residues that interact with sorbinil are shown in white and labelled with residue type and number. Trp 22, Tyr 50, His 113, and Arg 312 form hydrogen bonds with the sorbinil molecule. The hydrophobic residues Ile 49, Trp 82, Trp 114 and Phe 125 are within van der Waals contacts with the inhibitor. A long hydrogen bond may exist between Trp 114 and sorbinil. The side chains of Arg 312 and Asp 313 engage in a salt link. Atoms of inhibitor (right) and coenzyme (left) are color-coded according to type (O is red, C is black, N is blue, P is pink, S is yellow and F is green). Ribbon drawings were prepared using MOLSCRIPT [25].

ALR1 and ALR2 (Figure 2) is held in place by three salt bridges to residues Lys 23, Lys 263 and Arg 269 (the sequence numbering of ALR1 [6] is used in the study). The contribution of each amino acid residue adjacent to the coenzyme to the binding energy in ALR1 and ALR2 is shown in Table 1. In agreement with the crystal structures [7,8], with the exception of Asp 217, the estimated values of the intermolecular binding enthalpies in the two binary complexes are similar. A hydrogen bond previously noted in the crystal structures of ALR1 and ALR2 holoenzymes [7,8] between the 2'-hydroxyl of the nicotinamide ribose and the charged Asp 45 contributes the greatest to binding. Additionally, the stacking of Tyr 210 against the nicotinamide ring and the ionic interactions between Lys 263 and Arg 269 and the 2'-phosphate moiety make important contributions (>10.0 kcal/mol) to the binding of NADPH to ALR1 and ALR2. An important difference that exists between the coenzyme-binding residues of ALR1 and ALR2 is the non-conserved Ser 216 (Pro in ALR2). In ALR1, the hydroxyl of Ser 216 forms a hydrogen bond with the 3'-hydroxyl of the adenosine ribose. In ALR2, however, Pro 216 cannot form a hydrogen bond and instead a hydrogen bond present between the carboxylate of Asp 217 and the 3'-hydroxyl of the adenosine ribose makes an important contribution to the binding (Table 1). The rigid side chain of Pro 216 in ALR2 stacks against the adenosine ribose (3.6 Å apart) inducing a shift in the position of the adenosine-2'-phosphate moiety, which is likely stabilizing the hydrogen bonding interaction between Asp 217 and the coenzyme.

The interaction of ALR1 and ALR2 with NADPH differs in certain regions such that the binding of coenzyme to ALR2 is 10-fold tighter compared to ALR1 [11,12]. Pro 216 in ALR2 (Ser in ALR1) was mutated to a serine residue in order to investigate the effect of the non-conserved Pro 216 on the binding of coenzyme. The P216S mutation had little effect on the K_m value of NADPH (1.5x wildtype). A more direct effect can be seen by comparing the binding constants of NADPH with wildtype and P216S enzymes, where there is a 5-fold increase due to the mutation (Table 2), making the binding of NADPH with the P216S mutant more similar to that of ALR1. A similar effect was obtained with the oxidized coenzyme, $NADP^+$. Based on the criteria suggested by Tsai and Yan [21], when a 5-fold perturbation in kinetic parameters is supported by structural evidence, the mutated residue is considered to play a functional role provided the conformation of the mutant enzyme is not significantly perturbed relative to wild-type (in the free form and in complex with substrate). The diminished binding of NADPH to the P216S mutant may have resulted from the disruption of the hydrogen bond observed in the wild-type enzyme between the carboxylate of Asp 217 and the 3'-hydroxyl of the adenosine ribose nicotinamide.

The effect of the P216S mutation on the catalytic efficiency (k_{cat}/K_m) of the aldehyde substrate DL-glyceraldehyde (1.3x wildtype) was small, suggesting that the mutation does not affect the tertiary structure and the ability of the enzyme to reduce DL-glyceraldehyde. On the other hand, the increase in k_{cat} (3.8x) observed for NADPH and glyceraldehyde with the P216S mutation is an indication that the mutation has altered the active site to an extent that the release of $NADP^+$ and the product are affected.

Inhibitor-binding site: Sorbinil binds to the active site of the ALR1 holoenzyme (Figure 3) making 60 contacts with the protein and 10 contacts with the coenzyme (<4.0 Å distances). With the exception of the non-conserved Arg 312 (missing in ALR2 sequences [6]), the contacts are made by the six apolar residues: Trp 22, Ile 49, Tyr 50, Trp 82, His 113, and Phe 125. The corresponding residues in ALR2 (Trp 20, Val 47, Tyr 48, Trp 79, His 110, and Phe 122) have been reported to make similar interactions with sorbinil [22]. The ring system of sorbinil stacks against the side chain of Trp 22, making the largest number of contacts (28 in ALR1 and 29 in ALR2), while the non-conserved Arg 312 makes the least number of contacts with the inhibitor (4 in ALR1). Similar to ALR2 [22], the side chains of Tyr 50 and His 113 are within hydrogen bonding distance with the two carbonyl oxygens of the spirohydantoin ring of sorbinil and the side chain of Trp 22 forms a hydrogen bond with the fluorine atom of the inhibitor (Figure 4). A long hydrogen bond may exist between the Nε1 of Trp 114 and the carbonyl oxygen of sorbinil. Furthermore, a non-conserved hydrogen bonding interaction is present be-

Table 2. Kinetic constants of wildtype and mutant ALR2

Substrate	Wildtype	P216S	P216S/Wildtype
DL-Glyceraldehyde			
Km (mM)	0.053 ± 0.008	0.161 ± 0.027	3.0
kcat (s-1)	1.19 ± 0.12	4.49 ± 0.48	3.8
kcat/Km (s-1 M-1)	22700 ± 3450	29000 ± 8320	1.3
NADPH			
Kd (nM)	7.4 ± 1.4	37.7 ± 6.4	5.1
Km (mM)	13.3 ± 1.8	19.7 ± 5.0	1.5
kcat (s-1)	0.9 ± 0.1	3.4 ± 0.8	3.8
kcat/Km (s-1 M-1)	65200 ± 5200	185000 ± 66200	2.8
$NADP^+$			
Kd (nM)	5.8 ± 0.7	31.3 ± 6.1	5.4

Kinetic constants are expressed as mean ± S.D. for 3 and 4 replicate experiments for determining Kd, and Km and kcat values, respectively. Km and kcat for NADPH were determined using 10 mM glyceraldehyde as substrate.

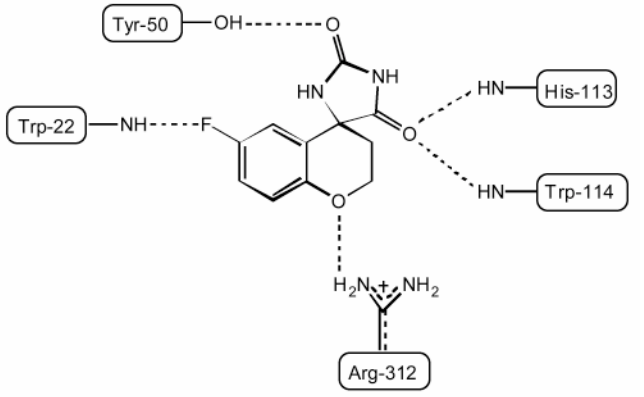

Figure 4. Chemical structure of sorbinil and the hydrogen bonding interactions with ALR1. With the exception of Arg 312 the sorbinil binding residues are conserved in ALR1 and ALR2. Hydrogen bonds between ALR1 and sorbinil are shown as dashed lines.

tween the non-conserved Arg 312 of ALR1 and the oxygen of the ring system of sorbinil. Thus, most of the interactions between the sorbinil molecule and the two enzymes are conserved.

The active site exists in a region with the least conserved residues [7] and is lined in part by an eight residue insertion segment (residues 306-313) from the C-terminal loop of ALR1. The binding of sorbinil to ALR1 does not induce a conformational change in the side chain of Arg 312, which is held in place by a salt link to Asp 313. However, unlike sorbinil, we have shown earlier that the binding of tolrestat is accompanied by a conformational change in the side chain of Arg 312, creating space for the inhibitor molecule to bind to the active site of ALR1 [9]. It is interesting to note that while mutation of Arg 312 to Ala increases the potency of inhibition by tolrestat, it has a less marked effect on sorbinil inhibition [23]. Thus Arg 312 is an important residue in the inhibitor binding site of ALR1 that by changing conformation allows the enzyme to bind to different ALR2 inhibitors. Similar to ALR1, the binding of sorbinil does not induce structural changes in ALR2. In the case of tolrestat, however, the side chains of Phe 122 and Leu 300 (Phe 125 and Pro 301 in ALR1) move allowing the inhibitor to bind to the active site [22]. A comparison of the crystal structures of the binary and ternary complexes of ALR1 and ALR2 indicates that the binding of inhibitor to the enzymes does not induce significant structural changes in the coenzyme-binding site [9,22,24].

The difference in the potency of inhibition by sorbinil and tolrestat for ALR1 and ALR2 is reflected in the mode of their interaction with the enzymes. While sorbinil inhibits both ALR1 and ALR2 with similar IC_{50} values [10] (5.4 μM and 2 μM for ALR1 and ALR2, respectively), tolrestat is a more potent inhibitor of ALR2 than ALR1 [10] (IC_{50} values of 0.72 μM and 0.01 μM for ALR1 and ALR2, respectively). In ALR2, the non-conserved C-terminal loop residues Ser 302 and Cys 303 form an extra four hydrogen bonds with the bound tolrestat while the side chain of Leu 300 (Pro 301 in ALR1) interacts through van der Waals contacts with the hydrophobic domain of the inhibitor [22]. Additionally, in ALR1 there are likely energy penalties accompanying the rearrangement in the side chain conformation of Arg 312 due to the loss of the salt link between Arg 312 and the neighboring Asp 313 that occurs upon tolrestat binding [9]. The participation of non-conserved residues from the C-terminal loop in the binding of tolrestat in addition to the differences in the structural changes required in order for the binding to occur are responsible for the 70 fold difference in the potency of inhibition of ALR1 and ALR2 [10]. On the other hand, the similar IC_{50} values of ALR1 and ALR2 for sorbinil [10] are due to the high homology in the interactions between the enzymes and inhibitor, which also involve the participation of non-conserved residues from the C-terminal loop but to a smaller extent.

ACKNOWLEDGEMENTS

We thank Sharon Kiang and Julia Birch (NIH) for technical assistance. This work was supported in part by the Australian National Health and Medical Research Council, Australian Research Council Small Grants Scheme and Monash University Research Fund (OEL-K). The Argonne National Laboratory Structural Biology Center at beamline X8C of the National Synchrotron Light Source is supported by the US Department of Energy, Office of Health and Environmental Research, under contract No. W-31-109-ENG-38.

REFERENCES

1. Flynn TG. Aldehyde reductases: monomeric NADPH-dependent oxidoreductases with multifunctional potential. Biochem Pharmacol 1982; 31:2705-12.
2. Kinoshita JH, Nishimura C. The involvement of aldose reductase in diabetic complications. Diabetes Metab Rev 1988; 4:323-37.
3. Speilberg SP, Shear NH, Cannon M, Huston NJ, Gunderson K. In-vitro assessment of a hypersensitivity syndrome associated with sorbinil. Ann Intern Med 1991; 114:720-4.
4. Sarges R, Oates PJ. Aldose reductase inhibitors: recent developments. Prog Drug Res 1993; 40:99-161.
5. Srivastava SK, Petrash JM, Sadana IJ, Ansari NH, Partridge CA. Susceptibility of aldehyde and aldose reductases of human tissues to aldose reductase inhibitors. Curr Eye Res 1982-83; 2:407-10.
6. El-Kabbani O, Green NC, Lin G, Carson M, Narayana SVL, Moore KM, Flynn TG, DeLucas LJ. Structures of human and porcine aldehyde reductase: an enzyme implicated in diabetic complications. Acta Crystallogr D Biol Crystallogr 1994; 50:859-68.
7. El-Kabbani O, Judge K, Ginell SL, Myles DA, DeLucas LJ, Flynn TG. Structure of porcine aldehyde reductase holoenzyme. Nat Struct Biol 1995; 2:687-92.
8. Wilson DK, Bohren KM, Gabbay KH, Quiocho FA. An unlikely sugar substrate site in the 1.65 A structure of human aldose reductase holoenzyme implicated in diabetic complications. Science 1992; 257:81-4.
9. El-Kabbani O, Carper DA, McGowan MH, Devedjiev Y, Rees-Milton KJ, Flynn TG. Studies on the inhibitor-binding site of porcine aldehyde reductase: crystal structure of the holoenzyme-inhibitor ternary complex. Proteins 1997; 29:186-92.
10. Barski OA, Gabbay KH, Grimshaw CE, Bohren KM. Mechanism of human aldehyde reductase: characterization of the active site pocket. Biochemistry 1995; 34:11264-75.
11. Kubiseski TJ, Flynn TG. Studies on human aldose reductase. Probing the role of arginine 268 by site-directed mutagenesis. J Biol Chem 1995; 270:16911-7.
12. Davidson WS, Flynn TG. Kinetics and mechanism of action of aldehyde reductase from pig kidney. Biochem J 1979; 177:595-601.
13. Westbrook EM, Naday I. Charge-coupled device-based area detectors. Methods Enzymol 1997; 276:244-68.
14. Messerschmidt A, Pflugrath JW. Crystal orientation and X-ray pattern prediction routines for area-detector diffractometer systems in macromolecular crystallography. Journal of Applied Crystallography 1987; 20:306-15.
15. Jones TA. (1985) Diffraction methods for biological macromolecules. Interactive computer graphics: FRODO. Methods Enzymol 1985;115:157-71.
16. Brunger AT, Krukowski A, Erickson JW. Slow-cooling protocols for crystallographic refinement by simulated annealing. Acta Crystallogr A 1990;46:585-93.
17. Jones DH, Howard BH. A rapid method for site-specific mutagenesis and directional subcloning by using the polymerase chain reaction to generate recombinant circles. Biotechniques 1990; 8:178-83.
18. Carper DA, Hohman TC, Old SE. Residues affecting the catalysis and inhibition of rat lens aldose reductase. Biochim Biophys Acta 1995; 1246:67-73.

19. Hohman TC, El-Kabbani O, Malamas MS, Lai K, Putilina T, McGowan MH, Wang YQ, Carper DA. Probing the inhibitor-binding site of aldose reductase with site-directed mutagenesis. Eur J Biochem 1998; 256:310-6.
20. Bradford MM. A rapid and sensitive method for quantitation of microgram quantities of protein utilizing the principle of protein-dye binding. Anal Biochem 1976; 72:248-54.
21. Tsai MD, Yan HG. Mechanism of adenylate kinase: site-directed mutagenesis versus X-ray and NMR. Biochemistry 1991; 30:6806-18.
22. Urzhumtsev A, Tete-Favier F, Mitschler A, Barbanton J, Barth P, Urzhumtseva L, Biellmann JF, Podjarny AD, Moras D. A 'specificity' pocket inferred from the crystal structures of the complexes of aldose reductase with the pharmaceutically important inhibitors tolrestat and sorbinil. Structure 1997; 5:601-12.
23. Barski OA, Gabbay KH, Bohren KM. The C-terminal loop of aldehyde reductase determines the substrate and inhibitor specificity. Biochemistry 1996; 35:14276-80.
24. Wilson DK, Tarle I, Petrash JM, Quiocho FA. Refined 1.8 A structure of human aldose reductase complexed with the potent inhibitor zopolrestat. Proc Natl Acad Sci U S A 1993; 90:9847-51.
25. Kraulis PJ. MOLSCRIPT: a program to produce both detailed and schematic plots of protein structures. Journal of Applied Crystallography 1991; 24:946-50.